Received: 17 March 2023 | Revised: 20 June 2023 | Accepted: 26 June 2023

DOI: 10.1111/nzg.12373

RESEARCH ARTICLE

NEW ZEALAND GEOGRAPHER WILEY

Interferometric Synthetic Aperture Radar (InSAR) and field-based observations of rainfall-triggered landslides from the November 2021 storm, Gisborne/Tairāwhiti, New Zealand

Matt Cook[1] | **Martin Brook**[1] | **Murry Cave**[2]

[1]School of Environment, University of Auckland, Auckland, New Zealand

[2]Gisborne District Council, Gisborne, New Zealand

Correspondence
Martin Brook, School of Environment, University of Auckland, Private Bag 92019, Auckland 1010, New Zealand.
Email: m.brook@auckland.ac.nz

Funding information
Earthquake Commission, Grant/Award Numbers: 1965/20799, 18/770

Abstract

Gisborne/Tairāwhiti is particularly susceptible to rainfall-triggered landslides on account of (1) steep slopes, (2) young, soft geology, (3) landuse change effects. The interplay of these factors led to a particularly damaging rainfall-induced landsliding event during 3–7 November 2021, following >200 mm of rainfall. This caused a Multiple Occurrence Regional Landslide Event, impacting residential properties and infrastructure in the city and rural areas. We report mainly on landslides in Gisborne city and suburbs, based on field reconnaissance and interferometric synthetic aperture radar monitoring of slopes. This highlights prevailing land instability prior to the more recent ex-Tropical Cyclone Gabrielle (2023).

KEYWORDS

Gisborne, land use, landslide, New Zealand, rainfall-triggering

1 | INTRODUCTION

In Aotearoa-New Zealand, Multiple Occurrence Regional Landslide Events (MORLEs) are the most common form of landsliding, occurring several times per year (Crozier, 2005). A single event can involve 1000 to 10,000s of individual landslides occurring almost simultaneously, over areas ~20,000 km^2. While a MORLE can result from an earthquake (e.g., Massey et al., 2020), most often MORLEs are rainfall-triggered, associated with an extra-tropical cyclone. Indeed, the critical rainfall intensity triggering slope failure is controlled by prevailing antecedent soil moisture conditions and/or rainfall duration (Crozier, 2005). The widespread nature of landsliding in a MORLE means it is challenging to analyse landslides using conventional ground-based surveying (Crozier, 2005). In recent years, Interferometric Synthetic Aperture Radar (InSAR) has emerged as a key remote sensing approach to allow areas to be rapidly surveyed without exposing people or equipment to risk, and can provide millimetre-scale measurements of Earth's surface deformation (Samsonov et al., 2020; Wasowski & Bovenga, 2014).

Gisborne, on the northeast of the North Island, with steep slopes, narrow ridgelines and clay-rich soils, is particularly susceptible to rainfall-triggered MORLEs (Cook, Brook, Tunnicliffe, et al., 2022). These landslides are often manifested as shallow flows within soil (Cumberland, 1944), as well as slow-moving slumps, which transition down-slope into earthflows during extreme rainfall (Cook, Brook, Tunnicliffe, et al., 2022; Tan, 2023). With summer rainfall

predicted to increase due to climate change on the east of the North Island (Bodeker et al., 2022), understanding rainfall-triggered landslides in the region is important. Here, we use Sentinel-1 data and InSAR processing techniques to determine the seasonal and annual slope velocity changes in suburban Gisborne from 2016 to 2021, in the lead-up to the damaging 3–7 November 2021 rainfall event (e.g., MacManus, 2021). We couple this with site reconnaissance surveys of landslide characteristics, as well as Sentinel-2 optical imagery of selected rural areas.

2 | STUDY AREA

Gisborne city is mainly on the Poverty Bay Flats, an alluvial floodplain of Waipaoa River (Figure 1). Surrounding the flood plain are steep hills <800 m above sea level, and these slopes are notorious for high erosion rates and changes in vegetation cover that has influenced erosion and landsliding in the soft sedimentary rocks (Marden, 2004). The geomorphology and geology of Gisborne is unequivocally controlled by the close proximity to the Hikurangi Subduction Margin, with the subduction of the Australian Plate causing regional uplift rates of the order of 1–4 mm/year (Berryman et al., 2010). Urban and suburban Gisborne is also affected by drainage from the Waimata River, which flows through the city from the northeast, into which incised gullies and tributary streams drain. Neogene units around the city and suburbs include mid to late-Miocene Tolaga Group mudstones and sandstones, and early Pliocene Mangaheia Group mudstones (Figure 1).

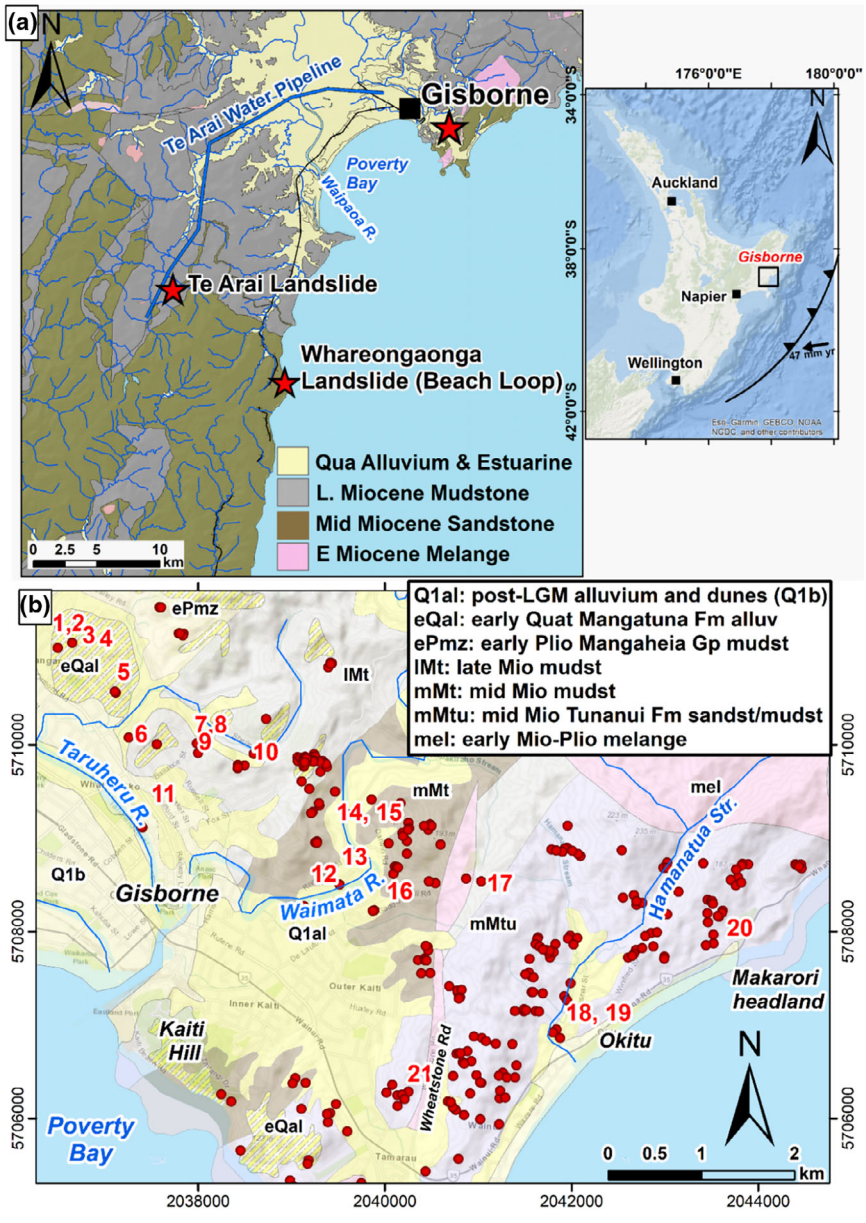

FIGURE 1 (a) Simplified geology of the Gisborne region with Te Arai and Whareongonga landslides also shown; (b) landslides (red circles) following the November 2021 storm in and around Gisborne city and suburbs (numbers are landslides visited and reported in Table 1), and geological abbreviations are from Mazengarb and Speden (2000).

The Quaternary Mangatuna Formation (Neef et al., 1996) typically comprises uplifted estuarine deposits, and includes clays, tephra and weak sandstones and mudstones. Importantly, the Mangatuna Formation is commonly associated with shallow soil failures in the city and suburbs when exposed on slopes by removal of vegetation cover, for example, on Kaiti Hill (Mazengarb, 1997). Nevertheless, slope instability in Gisborne is controlled by a range of factors, including smectite-rich surface soils and weak rocks, steep slopes, undercutting of slopes, and discontinuity orientations. A further factor is that often landslides represent reactivations of historic or prehistoric failures (Cook, Brook, Tunnicliffe, et al., 2022). While the majority of recorded landslides in Gisborne occur as flows or slump-flows in shallow soil, there is evidence of more deep-seated failures within rock (Mazengarb, 1997). Motion at Wallis Road landslide is partly facilitated by reactivated slip surfaces within the highly weathered Mangatuna Formation (Cook, Brook, Tunnicliffe, et al., 2022), and similar failure styles occur on other slopes in Kaiti and the Whataupoko suburbs (Figure 1), sometimes on slopes of ~5°.

Extreme rainfall events over the last few decades have caused MORLEs (c.f. Crozier, 2005), including ex-tropical cyclone Bola in 1988 (Franks, 1988), the Labour Weekend storm in 2005 (Beetham & Grant, 2006), ex-tropical cyclones Debbie and Cook in 2017 (Cook, Brook, Tunnicliffe, et al., 2022), and a slow-moving tropical storm in November 2021, which brought >250 mm over 3–7 November (Figure 2), the focus of this study. The highest rainfall totals for the November 2021 event were recorded in the Wharerata Ranges (377 mm) to the south of Gisborne near the Whareongaonga coastal landslide (Figure 2b). The 3–7 November 2021 event contributed to

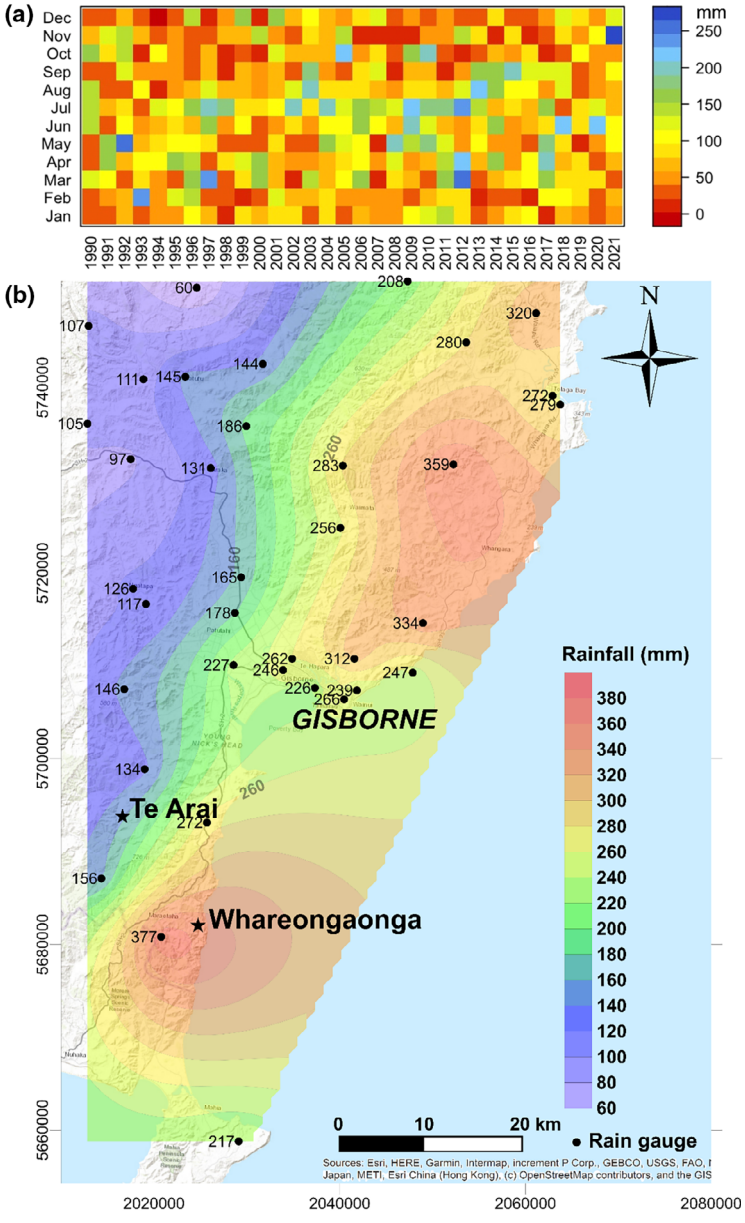

FIGURE 2 (a) Monthly rainfall totals for Gisborne airport automatic weather station 1990–2021, illustrating the magnitude of the 3–7 November 2021 event. Gisborne's 1990–2020 mean annual rainfall is 995 mm; 250.7 mm fell 3–7 November 2021; (b) Rainfall distribution for the November 3–7 2021 storm. Rainfall data provided by Gisborne District Council.

a monthly rainfall total unprecedented in the previous three decades (Figure 2a). The most damaging landslides occurring after the November 2021 storm within Gisborne city are displayed in Figure 1b. The event was manifested by >280 (1) shallow landslides within Gisborne city and suburbs (Figure 3), (2) thousands of shallow landslides in isolated, rural hill country, and (3) reactivation of several large landslide 'complexes' in the wider region. Specific examples of the latter are near the Te Arai water pipeline, 25 km southwest of Gisborne, as well as the coastal landslide that damaged the Wairoa-Gisborne rail line at Whareongaonga, 30 km south of Gisborne (Figure 1a).

However, these rural landslides are not the focus of the present study, which is restricted to Gisborne city and outlying suburbs in the November 2021 storm event.

FIGURE 3 (a and b) Slump-flow at Clifford Street undermining deck, tilting swimming pool; (c and d) Ballance Street fill/retaining wall failure, where cantilever embedded pole retaining wall has rotated; (e) Gaddum's Hill Road earthflow downslope towards 17 Darwin Road; (f) retaining wall failure at Owen Road above Waimata River; (g) scarplet and offset retaining wall from low angle slump at Argyll Street; (h) shallow earthflows at Wheatstone Road.

Notably, more recent storm events in the Gisborne region have also occurred (e.g., https://cliflo.niwa.co.nz/), including the 22 March 2022 storm (250–300 mm of rainfall over 24 h), 10–11 January 2023 ex-Tropical Cyclone Hale (~157 mm of rain in 12 h), and ex-Tropical Cyclone Gabrielle on 13–14 February 2023 (488 mm over 24 h at Hikuwai north of Gisborne). Therefore, the present study provides clear documentary evidence of urban landslides that occurred prior to the 2022 and 2023 storms, and which should therefore be excluded from the 2023 landslide inventory. However, the population of landslides catalogued here may prove useful in future studies of landslide reactivation during the 2023 storm events.

3 | METHODS

A site reconnaissance of Gisborne city and outlying suburbs was undertaken in the week following the 3–7 November 2021 storm to study failure modes, extent and characteristics. This was part of the State of Emergency response to assist Gisborne District Council in 'triaging' the impacted residential properties within the context of the Building Act (2004) section 124 (which relates to dangerous, affected or insanitary buildings; 'red' and 'yellow' stickering). For the InSAR analysis, the small baseline subset (SBAS) technique (Berardino et al., 2002; Li et al., 2022) was used to identify landslide-related slope displacement within the study area. Sentinel-1 single look complex images (12 or 24 day revisit cycle) from the interferometric wide-swath mode acquired from January 2016 to December 2021 for descending and ascending orbit directions were used (e.g., De Luca et al., 2022). From the ascending track 8, 163 images were used to generate a stack of 487 interferograms, and from the descending track 175, 137 acquisitions were used to generate a stack of 409 interferograms.

To reduce the temporal decorrelation, particularly between seasons, three connections per image were used. However, images from the winter months were used, which typically have a higher coherence, to produce several longer temporal interferograms to reduce the effects of fading signals and improve detection of long-term displacement (e.g., De Luca et al., 2022). Sentinel-1 images were processed using ISCE (e.g., Funning & Garcia, 2016), with displacement and time series obtained using MintPY (Zhang et al., 2019). With InSAR, the relationship between slope geometry and the satellite sensor is of high importance (Notti et al., 2014). Indeed, slope displacement can only be obtained if the dip orientation of the slope is parallel to the line of sight (LOS) of the satellite sensor (Colesanti & Wasowski, 2006). This is usually in an approximately westward (descending) or eastward (ascending) direction of the sensor (Notti et al., 2014).

Because for most landslides the displacement direction usually coincides with the direction of the steepest slope (Fookes et al., 2005), the accepted method to delineate the actual component of landslide movement (e.g., Notti et al., 2014) is to project the LOS velocity (V_{LOS}) along the direction of the slope (V_{SLOPE}). Thus, the V_{SLOPE} is determined via:

$$V_{SLOPE} = \frac{V_{LOS}}{C}, \quad (1)$$

where C is the coefficient derived from the LOS and downslope vectors in the north, east and upward directions. Positive V_{SLOPE} values are removed as they would represent uphill slope movement, points with $-0.2 < C < 0.2$ are also removed, as proposed by Notti et al. (2014), to improve precision. The coefficient, C, is calculated from the East (E), North (N) and Downslope (U) LOS vectors:

$$C = (E \times E_{SLOPE}) + (N \times N_{SLOPE}) + (U \times U_{SLOPE}). \quad (2)$$

The LOS vectors are a component of the heading angle (γ) and incidence angle (α) of the SAR sensor in radians, with the downslope vectors calculated from the aspect (a) and slope (s), following Notti et al. (2014). Selected InSAR velocity results were overlaid on a LiDAR hillshade acquired in 2019, as well as aerial imagery.

In addition to Sentinel-1 InSAR, to investigate the impact of the November 2021 storm event on erosion in rural parts of Gisborne, Sentinel-2 optical (5-day revisit cycle) imagery was also examined (Zhang et al., 2022). The Sentinel-2 imagery used here, near infrared, red, green, and blue bands have a spatial resolution of 10 m (Zhang et al., 2022). The Sentinel-2 images are from late-October 2021 and mid-November 2021, in two areas of particular interest, namely Wheatstone Road, and Makarori. Both areas are covered by grassy pasture, and were subject to shallow landsliding during the November 2021 storm. Slope angle is one of the most significant factors in landslide occurrence and is inversely connected to slope stability (Hearn et al., 2011). For each landslide, the top of the main scarp, the slide toe, and a polygon encompassing the landslide failure source area was mapped. The extent of each landslide was delineated by a polygon on the 2019 LiDAR, and the pixel with the steepest slope was identified following Dellow et al. (2005). This was used as the landslide initiation (or 'start') angle.

4 | RESULTS

Table 1 reports the field reconnaissance of twenty-one (21) selected landslides (denoted L#) from the Gisborne

TABLE 1 Summary of main urban and suburban slope failures from November 2021 storm event (see Figure 1 for locations), including start (i.e., initiation) angle (a_s°) and headscarp to toe length (L in m).

L#	Location	Landslide characteristics	A_s°	L m
L1	Winter St	Not reported until months later by neighbours reporting sediment discharge. Downhill of Argyll St, movement of unstable low angle failure; complete failure in March 2022 storm	15	38
L2	Argyll St	Large tension crack forming headscarp of shallow slump extending from 24 to 28 Argyll; worst affected 26 Argyll; major reactivation following March 2022 storm; runout/toe removal at 35 Winter St exacerbating factor	8	35
L3	Diana Drive	Slumping on boundary resulting from neighbour landscaping close to foot of retaining wall; exacerbated by weight of water in swimming pool close to edge	33	20
L4	Belgium Tce	Moderate-sized slip on boundary between #4 and adjacent property, no obvious contributing factors	38	40
L5	Massey Rd	Landslide on steep slope adjacent to garage; tree removal on slope a factor; debris impacting property on Oswald St below	28	30
L6	Clifford St	Significant landslide undermined deck at 371; stormwater discharge onto unstable slope & weight of swimming pool on edge of steep face contributed; s124 notice; debris & threat to 395 Clifford	36	70
L7	Hill Rd	Major landslide; large unconsented retaining wall and fill with poor drainage controls failed; blocked Hill Rd isolating occupant requiring urgent medical treatment; runout onto Ballance St	40	70
L8	Hill Rd	Significant tension crack with some slumping at edge of face at 194; risk to 194a&b; s124 notices issued	31	12
L9	Stanford Cres	Slumping of slope above house exacerbated by vibrations from truck unloading large digger on road reserve above slope.	27	13
L10	Richardson Ave	Reactivation of 2019 landslide; new cracking & slumping below ridgeline near house; swimming pool tilted; runout of earthflow constrained within gully	40	90
L11	Stout St	Slumping on land on riverbank caused by failure of stormwater system	42	15
L12	Owen St	Major slip on riverbank but above flood height; main driver ground saturation and elevated pore pressures in Matokotoki Member	45	29
L13	Island Rd	Slip on boundary of 29 & 27; contributing factors poor stormwater controls @ #29, elevated river levels and saturation of slope toe by river	37	25
L14	Riverside Rd	Small landslide on steep hill landed in creek; debris flow from creek discharged downhill onto property	46	150
L15	Riverside Rd	Small slip close to house as a result of undercutting by small stream on boundary	36	10
L16	Gaddums Hill Rd/ Darwin Rd	Major slip at 28 Gaddums Hill; swimming pool at edge of steep slope contributing factor (0.3 m setback); debris and threat to 17 Darwin Rd below; minimal setback	32	65

(Continues)

TABLE 1 (Continued)

L#	Location	Landslide characteristics	A_s°	L m
L17	Gaddums Hill Rd	Collapse of slope on road edge undermined power transformer; debris flow downslope with damaged fences on adjacent blocks; stormwater from adjacent houses a factor	33	40
L18	Williamson Stre	Failure on stream bank driven by flood height affecting toe	28	15
L19	Moana Rd	Failure on stream bank driven by flood height affecting toe; exacerbated by high levels of water flow from road culvert on headscarp	28	10
L20	Sirrah St	Collapse on bank close to house; blocked road isolating ill person	38	25
L21	Wheatstone Rd	Shallow slumping on southeast-facing slope; actively deforming for several years	45	82

city and suburbs visited the week following the November 2021 storm, that had particular impacts on residential property. The numbers in the first column of Table 1 correspond with the numbers on Figure 1b. The landslides exhibited typical characteristics of previous rainfall-triggered landslides in the Gisborne region. They are mainly shallow (<2 m) slumps on slopes with initiation angles (A_s) of 25–35°, that transition downslope into earthflows, with runout usually topographically-constrained within existing gullies. Material types that failed include fill (e.g., Hill Road, L8), fluvial deposits (e.g., Owen Street, L12), residual soils, and colluvium (e.g., Gaddums Hill Road, L16). Occasionally, the slope failures incorporated some highly-weathered rock (Richardson Avenue, L10). Some images of example November 2021 landslides are shown in Figure 3. In particular, Clifford Street landslide (L6) commenced as a rotational slump under the deck, then accelerated downslope as a flow, which inundated the rear of a property below (Figure 3a,b). Tilting of the swimming pool also occurred, and the additional effect of slope loading from the swimming pool may have contributed to slope instability.

A remarkable landslide occurred at the intersection of Hill Road and Ballance Street (Figure 3c,d). This was a fill failure, where the natural land surface had been extended southwest to accommodate a tennis court and floodlights, as 'made ground'. This was composed of locally-sourced soil as the fill, which was retained via a retaining wall consisting of embedded timber poles, with timber planks as the 'lagging'. The earthflow extended ~40 m down Ballance Street, across the road and grass verge. At the Darwin Road slump-earthflow, a swimming pool was also present immediately adjacent to the headscarp (Figure 3e). This landslide exhibited high mobility, extending >120 m downslope into a property on Darwin Road, below. Embedded timber poles in the retaining wall were exposed at Owen Road, where the riverbank below the property was under-cut, and slumped, and the retaining wall failed (Figure 3f).

In contrast to the typically more mobile earth flows, at Argyll Street a low angle slump initiated on a slope of ~12°, with the headscarp in a back garden, and displacement away from the house, downslope to the west (Figure 3g). Slope velocity was unwittingly accelerated somewhat by the downslope (adjacent) landowner excavating the toe of the slump. On the edges of suburban Gisborne, shallow earthflows occurred on pastureland, and typical examples are shown in grazing paddocks at Wheatstone Road (Figure 3g). These types of landslides are of growing importance in the Wheatstone Road area, due to the residential subdivisions that are being developed (e.g., landslide L21, Table 1).

In contrast to the above earthflows, examples of large volume landslide 'complexes' are shown in Figure 4. The ~0.17 km^2 Te Arai landslide, 24 km southwest of Gisborne is a large earthflow 'complex', and is ~700 m long and has an overall gradient of 18°. Failure is possibly facilitated by bedding planes in the underlying Tolaga Group mudstones (Figure 4b). In November 2021, the landslide terminated 30 m from the Te Arai water pipeline, which transfers the majority Gisborne's city water supply from Mangapoike Dams to the Waingake Water Treatment Plant. Unfortunately, subsequently during Cyclone Gabrielle in February 2023, the Te Arai pipeline was severely damaged by multiple landslide reactivation and associated mobilisation of large woody debris from adjacent forests, cutting off the majority of Gisborne's water supply (Sharma, 2023). The November 2021 storm also triggered large volume coastal landslides

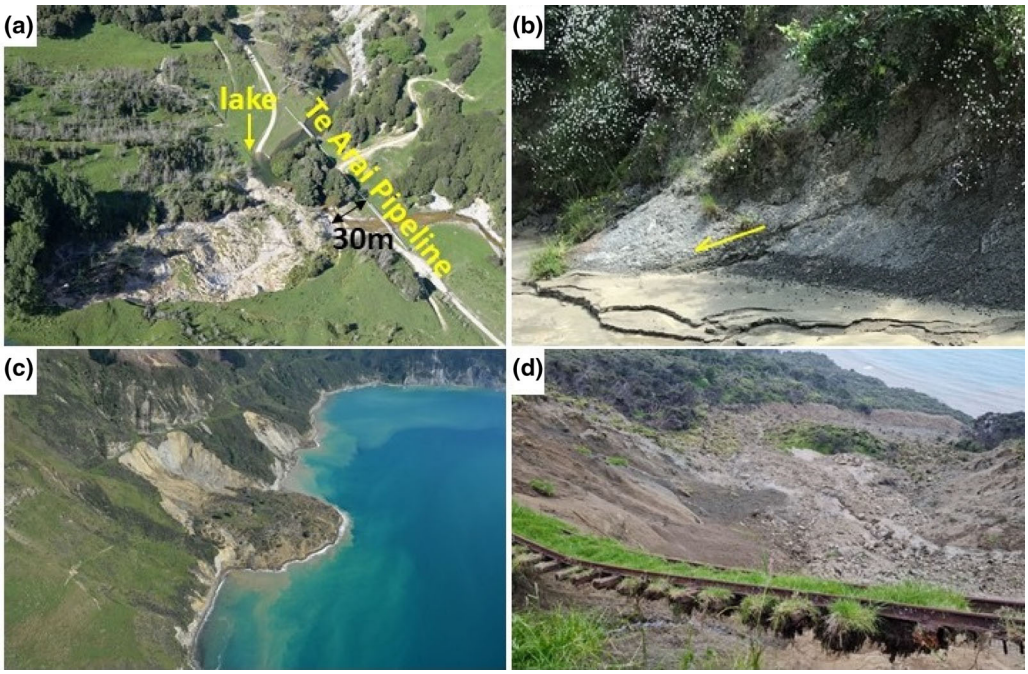

FIGURE 4 Large volume, rural landslide examples: (a) Te Arai landslide complex that reactivated and extended to ~30 from the Te Arai water pipeline, damming the Waingake/Te Arai River, forming a lake; (b) unfavourable mudstone bedding dip exposed near toe; (c) Whareongonga Landslide including (d) view from headscarp and undercut Wairoa-Gisborne railway line.

in the Tolaga Group sediments, and the Whareongaonga Landslide is one example (Figure 4c,d), ~30 km south of Gisborne. The landslide destroyed culturally important pā and fishing ground for Ngāi Tāmanuhiri. Rosser and Wolter (2022) reported 1.3 million m^3 of soil and rock was displaced by the November 2021 event, with runout below the intertidal zone. The landslide also undercut the Wairoa Gisborne railway line (Figure 4d).

In addition to the information gleaned from the field reconnaissance, Sentinel-2 optical satellite imagery was useful for regional-scale overviews of landsliding in the Wheatstone Road area east of Gisborne (Figure 5a,b), and around the coastal township of Makarori (Figure 5c,d). Indeed, comparing the pre-storm (October 2021) and post-storm Sentinel-2 imagery, linear pale hues are visible on the hill pasture perpendicular to the axes of ridgelines in the post-storm imagery, representing shallow earthflows. Sentinel-1 InSAR results showing annual average slope velocity (2016–2021) is also shown in Figure 6. As can be seen from the Figure 6 plots, most of the points analysed indicate that slopes are deforming at ~15–30 mm/year. A more detailed example of InSAR velocity of slopes around Wheatstone Road (landslide #21) is shown in Figure 7. This landslide is a shallow rotational slump, which transitions downslope into an earthflow (Figure 7a), but is also extending upslope by headscarp retrogression, towards a house. Parts of this landslide exhibit velocities of ~30 mm/year. Figure 7b shows the timeseries of slope velocity of landslide #21 from 2016 to 2021, with the groundwater fluctuations from a piezometer at Cameron Road also shown on the plot (blue line), together with monthly rainfall (blue bars). The velocity pattern (black line) shows that the slope is following a generally consistent annual pattern of movement, with large inflections in the trend due to major rainstorms, causing a pulse of rotational slumping to occur.

A seasonal trend is also present in the InSAR data. This represents annual shrinking (summer drying) and swelling (winter wetting) of the clay-rich soils. The piezometer record also shows that groundwater tracks rainfall input rather closely. Figure 7c shows the 2021 soil moisture deficit and modelled surface runoff from Niwa's Gisborne weather station (Agent 24976), along with the weekly Cameron Road piezometer record. As can be seen from Figure 7c, 2021 was a very dry year, and for the majority of the year until the November 2021 storm, the soils were very much in soil moisture deficit. Figure 7d reports the daily rainfall and cumulative daily rainfall record from the same Niwa station. This again confirms that 2021 was a year of below average rainfall and dry conditions. Until November 2021, Gisborne has only received 55% of its annual average total of 995 mm (based on the 1990–2020 'normal'). Moreover, despite the impact of the November 2021 storm, even by the year end, Gisborne had still only received 80% of its 1990–2020 annual average rainfall total (Figure 7d).

The 2019 LiDAR Sentinel-1 InSAR data also provides evidence for the reactivation of pre-existing landslides.

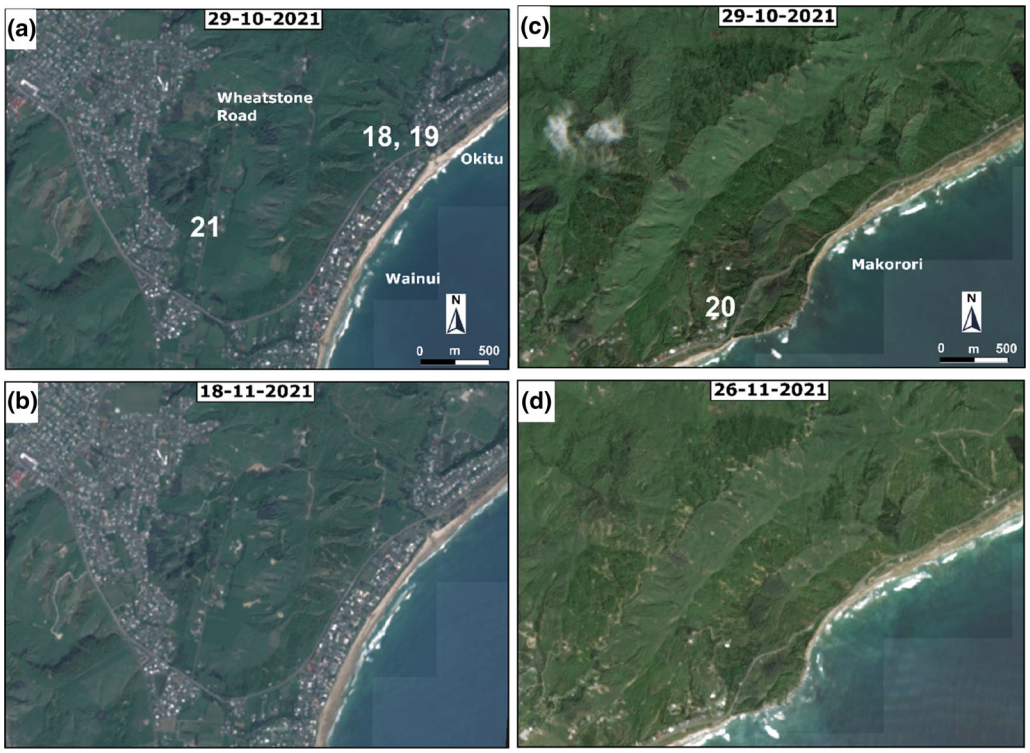

FIGURE 5 Sentinel-2 optical satellite imagery before and after the November 2021 storm event for the Wheatstone Road area (a and b) and Makorori (c and d).

An example is at Gaddums Hill Road (Figure 8). Indeed, the 2019 LiDAR digital elevation model reveals that several landslide headscarps are present along the north-facing ridgeline (Figure 8c). Below these landslide source areas, undulating topography on the slope is indicative of landslide debris. The InSAR data trendline (Figure 8d) shows that the slope velocity prior to swimming pool installation was at a rate of ~2–3 mm/year, and this rate continued until around early 2021. Since then, the slope appeared to show a very slight increase in velocity. In November 2021, the landslide (#16) initiated via rotational slumping adjacent to a swimming pool (installed early 2018), and transitioned in a mobile channelised earthflow, extending downslope onto the 17 Darwin Road property (Figure 8b). So, the November 2021 landslide (yellow hash in Figure 8c) was actually the reactivation of existing landsliding at the site. Thus, the Sentinel-1 InSAR is also useful in monitoring slope velocity in areas of existing landslides within urban Gisborne, that are vulnerable to reactivation.

5 | DISCUSSION

5.1 | Geomorphology and geology

A plethora of site pre-conditioning factors can contribute to landslide activity and reactivation of 'dormant' landslides (Crozier, 2010). The latter are where the slope has failed in the past, and the slope materials are then at a residual strength, which is lower than their original, peak strength, and may be more susceptible to failure (Stringer et al., 2021). Whether or not a slope fails in soil, rock or fill material is important, because soil and fill fail through the granular mass, while rock fails along defects such as joints and/or bedding planes (Hungr et al., 2014). Within the Gisborne area, as shown by site visits and Sentinel-2 optical imagery, shallow slumps and flows are common. Some of these are new failures, while others are more likely to be reactivated existing landslides. Generally, the observed landslides reported herein accord with previous observations of shallow landslides in the region, that typically occur within the highly-weathered Pleistocene Mangatuna Formation soils (e.g., Cook, Brook, Hamling, et al., 2022; Mazengarb, 1997; McKelvey & Murton, 1991). In addition, however, several failures have been reported on 'fill' slopes, where slopes have been modified to accommodate construction activity, such as tennis courts or swimming pools. Such fill failures are not uncommon across New Zealand, often due to poor compaction and drainage management in urban and suburban areas (e.g., Brook, 2018). Nevertheless, whether the landslide is within soil or fill, it is probably promoted by drainage and permeability contrasts that occur with the underlying Miocene Tunanui Formation mudstones (Cook, Brook, Hamling, et al., 2022). Such contrasts cause elevated groundwater tables during heavy, prolonged

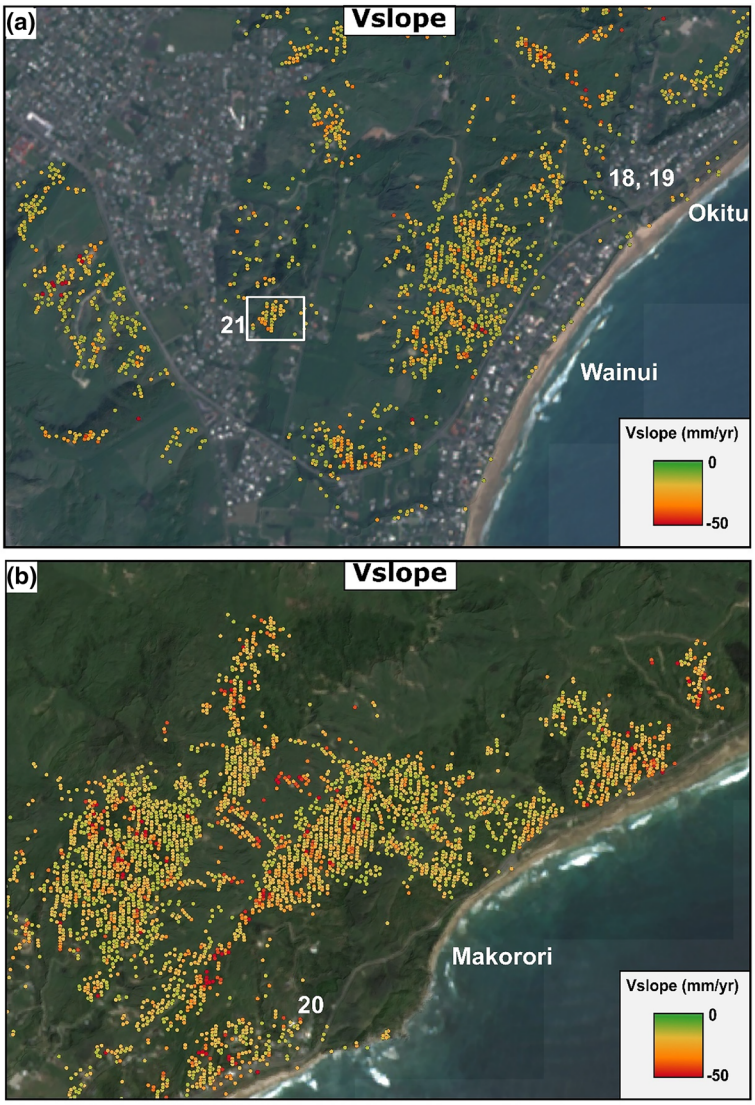

FIGURE 6 Sentinel-1 InSAR slope velocity (Vslope) data for January 2016 to December 2021 for the Wheatstone Road area (a) and Makorori (b). White box in (a) is the extent of the aerial image in Figure 7, including Landslide #21.

rainfall, as indicated by groundwater 'daylighting' out of exposed landslide headscarp exposures.

The Mangatuna Formation soils have an effective friction angle of ~30° (EQC, 2015), but if soil have undergone 'strain-softening' through modification, loading or landsliding, they may be at a lower residual strength, making them susceptible to failure (e.g., Bromhead, 1979). Hence, the residual friction angles of the soils are probably much lower than 30°, and close to typical slope angles. A further effect evident from the Sentinel-1 InSAR data affecting soil strength is the annual pattern of shrinking (drying) and swelling (wetting) of the clay-rich soils in the region. Field evidence for shrink-swell properties of the Mangatuna Formation soils at Wallis Road on the eastern slopes of Kaiti Hill was presented in Cook, Brook, Tunnicliffe, et al. (2022). These effects can have a further 'strain-softening' effect on soils, making them progressively weaker over time, and therefore more suspectable to failure (Skempton, 1964).

5.2 | Rainfall triggering thresholds

As outlined above, when rainfall infiltrates into a slope, there is an increase in porewater pressure, which leads to the reduction in material cohesion and internal friction, hence reduced shear strength of the slope material (Crozier, 2010). Rainfall thresholds represent the amount (e.g., in mm) of rainfall required to reach critical porewater pressures which initiates landslides, over a given measurement period (often 24, 48 or 72 h; Crozier, 2005). However, water content from a storm alone does not solely initiate shallow landslides, as pre-storm antecedent soil moisture conditions must be taken into account in

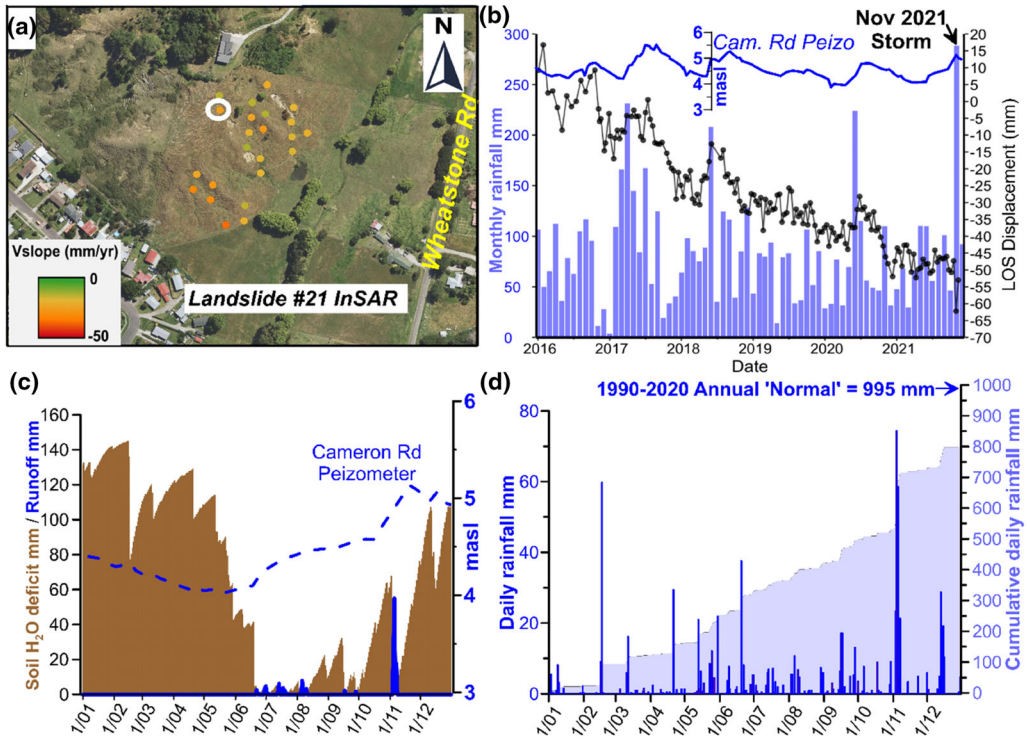

FIGURE 7 (a) aerial imagery (from 2017) of Wheatstone Road, that reactivated during November 2021 event (see Figure 6a for location); (b) time series of velocity in the LOS acquired from the point highlighted in the white circle in (b), plotted against total monthly rainfall. Cameron Road piezometer (blue line) is superimposed on the plot; (c) soil water deficit (brown bars) and runoff (blue bars) showing dry soil conditions in the months preceding the November 2021 storm, along with Cameron Road weekly piezometer record for 2021; (d) 2021 daily rainfall (blue bars) and cumulative daily rainfall (blue shade), with 1990–2020 mean annual ('normal') total 995 mm. All data from Gisborne Niwa Agent 24976 (https://cliflo.niwa.co.nz/).

the initiation of landsliding (Glade, 1998). Indeed, the interplay between rainfall events, antecedent rainfall, soil and bedrock properties makes it notoriously difficult to develop definitive rainfall thresholds above which slope failure is triggered (Ram et al., 2018).

Thus, rainfall thresholds for landsliding vary markedly across New Zealand (Crozier, 2010) for a myriad of reasons (Glade, 1998). Importantly, the rainfall that triggered Gisborne's landsliding in November 2021 was not the result of high-intensity rainfall over a few hours, as per the 27 January 2023 rainfall-triggered landsliding in Auckland (149.6 mm fell between 5 and 9 pm; NIWA, 2023), but was rather the result of cumulative rainfall (~250 mm) over five consecutive days. Thus, daily rainfall totals during the November 2021 Gisborne event were rather modest, and were individually well below the 24-h thresholds typical of regionally-significant landslide triggering events (Kluger et al., 2020). However, the moisture content of slope materials was gradually increasing over the 3–7 November period, eventually triggering landslides. Indeed, the global rainfall intensity-duration threshold suggested by Caine (1980), and subsequently updated by Sidle and Ochiai (2006) can be compared with the Gisborne November 2021 event, as follows:

$$I = \alpha D^{-\gamma}, \tag{3}$$

where I is the rainfall intensity (mm/h), D is the duration of rainfall (h), and $\alpha = 13.58$ and $\gamma = 0.38$ are the intercept and slope of the power-law function, respectively. The Gisborne 5-day total (~250 mm) would fall just below the critical rainfall-intensity-duration curve of the power-law in Equation 3, further reinforcing that the prevailing longer-term soil moisture conditions at the onset of the storm was of importance.

A further factor is the interplay between rainfall duration and the nature of the clay-rich Gisborne soils (Mazengarb, 1997; Neef et al., 1996). While antecedent rainfall and elevated soil moisture can be important (Crozier, 2010), in New Zealand slope failures often occur in Summer (Hancox & Wright, 2005) when the ground is drying out, soils are shrinking, and fissures through the soil mass have opened. This can result in slopes that are vulnerable to rainfall events that are not necessarily of

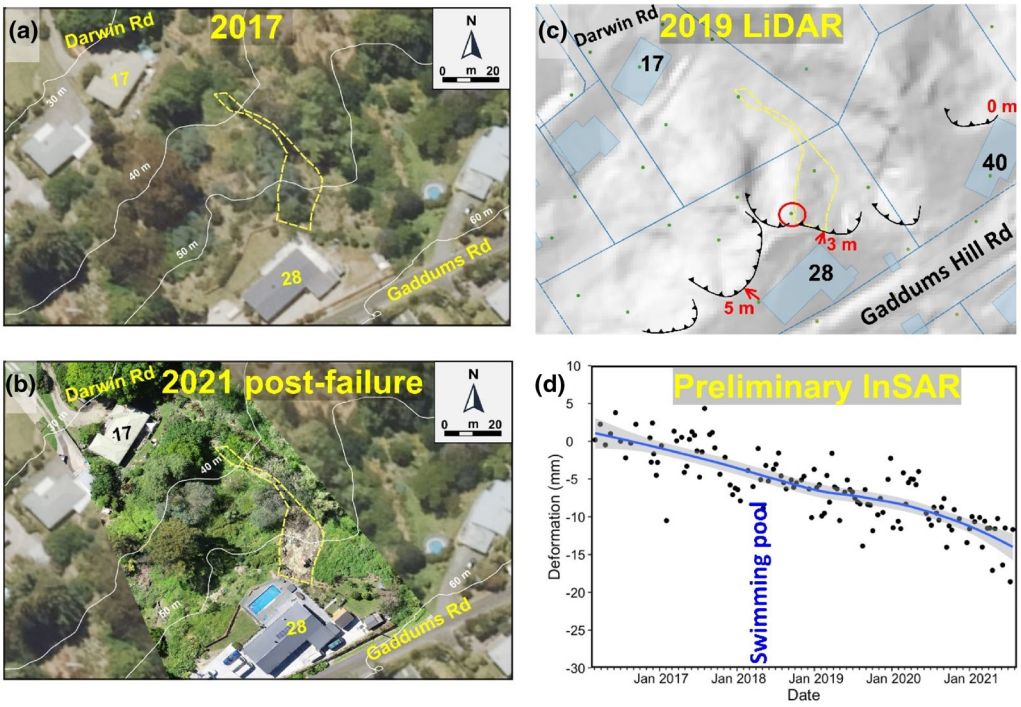

FIGURE 8 Slump-earthflow at Gaddums Hill Road, which flowed downslope from north end of swimming pool towards 17 Darwin Road (landslide #16, Table 1): (a) pre-failure imagery from 2017; (b) post-failure imagery from 2021; (c) 2019 pre-failure LiDAR showing existing landslide headscarp areas (black lines) and InSAR target (dot inside red circle); (d) 2016–2021 InSAR LOS displacement showing gradual downslope movement, with slight increase through 2021. Blue line is the 7-day rolling mean and grey shading is the 95% confidence interval.

high magnitude and intensity. The fissures allow water to infiltrate deeper and faster than when soils are more moist and fissures have narrowed (e.g., Rogers et al., 2022), in 'wet' periods. The monthly totals (Figure 2a) accord with this drying and fissuring effects in the clay-rich soils. Indeed, the cumulative rainfall total in Gisborne from 1 January to 31 October 2021 was only 532 mm. This is only 62% of the long-term average for January–October for Gisborne (~850 mm). The soil moisture deficit record for Gisborne in 2021 accords with this. Thus, the clay-rich soils prevalent in Gisborne (e.g., Mazengarb, 1997) would have been deeply fissured by shrinkage by November 2021. Rainfall then infiltrated rapidly down through the soil towards the underlying rock mass via fissures, creating temporary elevated 'perched' groundwater levels. It is possible this was key to initiating failures.

5.3 | Anthropogenic factors

Emerging evidence cautions that land-use change may equal, or in some instances exceed, the impact of climate change in affecting the temporal and spatial occurrence of landslides (Ozturk et al., 2022). Indeed, growth and land development for residential properties and related infrastructure often neglects the natural constraints that are bestowed by the local environment (Bozzolan et al., 2020). Thus, in addition to the rainfall outlined above, site-specific anthropogenic factors also appear to influence slope failures in the Gisborne region, namely: (1) vegetation removal, (2) inadequate slope stabilisation and drainage, (3) slope loading and (4) topographic changes/cutting. First, landsliding caused by vegetation removal in rural parts of the region due to forestry, has long been an issue in the region (Marden, 2004). However, removal of vegetation on slopes with the suburbs of Gisborne has also recently been identified as a key land stability issue (Cook, Brook, Hamling, et al., 2022), with tree cutting eliminating canopy cover, facilitating peak pore water pressure increases within soils (e.g., Keim et al., 2006). In addition, mechanical reinforcement of soils by roots is removed (e.g., Schwarz et al., 2013).

Second, slope stabilisation methods such as cantilever embedded pole retaining walls had also failed at some of the landslides studied here, implying inadequate design (Elkink, 2010). Failure of such walls preferentially occurs where pole embedment depth is inadequate, and the lateral load of saturated soil is then underestimated within the design (e.g., Wood, 2021). A related issue with poorly-designed retaining walls is inadequate drainage within the retaining wall (Xu & Zhang, 2010). Thus,

groundwater builds-up behind the retaining wall, increasing the weight of the soil mass, raising the water table and lateral earth pressure on the retaining wall (Elkink, 2016). Third, structures such as swimming pools placed on the edge of a slope act as a 'surcharge', adding vertical pressure to the slope (Li & Cheng, 2015). This surcharge load will result in additional horizontal pressure on a retaining wall, and is why appropriate construction 'setback distances' for swimming pools (e.g., 2.13 m; California Building Code, 2016) are applied diligently in jurisdictions in the USA (Olshansky, 1998). Some of the landslides observed in Gisborne were on slopes where a swimming pool had been installed close to the slope edge with negligible (0.5 m) setback, so slope failure was not unpredictable in such instances.

Finally, earthworks are the fourth aspect of anthropogenic effects on slope stability in Gisborne that are worth exploring here, albeit briefly. The roading network of the Tairāwhiti Region is so challenging that given the size of the roading network and the limited available funding, road operators expect only a 15-year design life for flood damage repairs (Fellows & Barker, 2021). Nevertheless, residential house-holders probably prefer more resilient slopes within their property boundaries. However, slope cutting and modification on steep sites does occur (e.g., slopes above Richardson Avenue), including infilling of tension cracks and earthworks to flatten landforms developing due to active landslides (Cook, Brook, Hamling, et al., 2022). Indeed, modification of slope morphology at that site included in-filling of tension cracks, and excavation of the stepped morphology formed from shallow rotational movements (e.g., Hearn et al., 2011), yet the slope remains active.

6 | CONCLUSIONS

The November 2021 rainfall event in Tairāwhiti/Gisborne caused widespread damage across the rural parts of the region, as well as Gisborne city itself. In many aspects, landslides generated during the event, typified previous rainfall-triggered MORLEs on soft, Neogene rock units on the North Island. Indeed, the sheer extent of the affected area as well as the number of landslides that occurred presented a management problem for the unitary authority (Gisborne District Council), distinctly different from typical site-specific slope instability problems in the region. Nevertheless, the style of landslides that occurred in Gisborne city and suburbs was typical of those reported previously from rainfall-triggered landslides in the area. Indeed, the landslides tend to be shallow (<2 m), seated in surface soils, which become saturated due to the lower permeability of the underlying weathered mudstone and clays, which act as an infiltration barrier. The pore water pressure in the surface soils increases following rainwater input, lowering the effective stress, and triggering failure. Notwithstanding this, landslides during the November 2021 event were in-part due to the unusual prevailing elevated antecedent moisture conditions, rather than a single short duration, high intensity (e.g., 24-h) rainfall event. A range of landslide preconditioning factors are evident, and these relate to land use change (i.e. vegetation removal, slope modifications) and slope management (inadequate retaining structures and drainage). Sentinel-1 InSAR has proven useful in detecting slope velocity changes as well as annual cycles of shrinking and swelling of the clay-rich soils, due to seasonal wetting and drying. The Sentinel-2 optical imagery was also useful in detecting rainfall-triggered landsliding at a sub-regional scale across pasture.

ACKNOWLEDGEMENTS

The authors thank Gisborne District Council (GDC) and the Earthquake Commission (EQC) for facilitating this work (grants EQC 18/770 and 1965/20799). The risk management teams at GDC and the University of Auckland are acknowledged for expediting the provision of travel exemption documentation to cross the Auckland border checkpoints during the COVID-19 lockdown. Open access publishing facilitated by The University of Auckland, as part of the Wiley - The University of Auckland agreement via the Council of Australian University Librarians.

DATA AVAILABILITY STATEMENT

The data that support the findings of this study are available from the corresponding author upon reasonable request.

ORCID

Martin Brook https://orcid.org/0000-0002-1030-3246

REFERENCES

Beetham, R. D., & Grant, H. (2006). Reconnaissance of landslide and flood damage in the Gisborne area caused by the 2005 Labour Weekend storm. GNS Science Report 2006/022, 35 p.

Berardino, P., Fornaro, G., Lanari, R., & Sansosti, E. (2002). A new algorithm for surface deformation monitoring based on small baseline differential SAR interferograms. *IEEE Transactions on Geoscience and Remote Sensing*, *40*, 2375–2383.

Berryman, K., Marden, M., Palmer, A., Wilson, K., Mazengarb, C., & Litchfield, N. (2010). The post-glacial downcutting history in the Waihuka tributary of Waipaoa River, Gisborne district: Implications for tectonics and landscape evolution in the Hikurangi subduction margin, New Zealand. *Marine Geology*, *270*, 55–71.

Bodeker, G., Cullen, N., Katurji, M., McDonald, A., Morgenstern, O., Noone, D., Renwick, J., Revell, L., & Tait, A. (2022). Aotearoa New Zealand climate change projections guidance: Interpreting the latest IPCC WG1 report findings. Prepared for the Ministry for the Environment, Report number CR 501, 51 p.

Bozzolan, E., Holcombe, E., Pianosi, F., & Wagener, T. (2020). Including informal housing in slope stability analysis – An application to a data-scarce location in the humid tropics. *Natural Hazards and Earth System Sciences*, *20*, 3161–3177.

Bromhead, E. N. (1979). A simple ring-shear apparatus. *Ground Engineering*, *12*, 40–44.

Brook, M. S. (2018). Field reconnaissance of the Rawene Slip urban landslide, Auckland, New Zealand. *Landslides*, *15*, 2295–2302.

Building Act. (2004). *Ministry of business innovation and employment*. New Zealand government.

Caine, N. (1980). The rainfall intensity-duration control of shallow landslides and debris flows. *Geografiska Annaler*, *62A*, 23–27.

California Building Code. (2016). *California code of regulations title 24, Volume 1 & 2*. Building Standards Commission.

Colesanti, C., & Wasowski, J. (2006). Investigating landslides with space-borne Synthetic Aperture Radar (SAR) interferometry. *Engineering Geology*, *88*, 173–199.

Cook, M., Brook, M. S., Tunnicliffe, J., Cave, M., & Gulick, N. (2022). Preliminary investigation of emerging suburban landsliding in Gisborne, New Zealand. *Quarterly Journal of Engineering Geology and Hydrogeology*, *55*. https://doi.org/10.1144/qjegh2021-087

Cook, M. E., Brook, M. S., Hamling, I. J., Cave, M., Tunnicliffe, J. F., Holley, R., & Alama, D. (2022). Engineering geomorphological and InSAR investigation of an urban landslide, Gisborne, New Zealand. *Landslides*, *19*, 2423–2437. https://doi.org/10.1007/s10346-022-01938-z

Crozier, M. (2005). Multiple-occurrence regional landslide events in New Zealand: Hazard management issues. *Landslides*, *2*, 247–256.

Crozier, M. (2010). Landslide geomorphology: An argument for recognition, with examples from New Zealand. *Geomorphology*, *120*, 3–15.

Cumberland, K. B. (1944). *Soil erosion in New Zealand*. Soil Conservation & Rivers Control Council.

De Luca, C., Casu, F., Manunta, M., Onorato, G., & Lanari, R. (2022). Comments on "Study of Systematic Bias in Measuring Surface Deformation With SAR Interferometry". *IEEE Transactions on Geoscience and Remote Sensing*, *60*, 1–5.

Dellow, G. D., McSaveney, M. J., Stirling, M. W., & Berryman, K. R. (2005). A probabilistic landslide hazard model for New Zealand (abs). In J. R. Pettinga & A. M. Wandres (Eds.), *Geological Society of New Zealand 50th annual conference, 28 November to 1 December 2005*. Kaikoura: programme & abstracts, Geological Society of New Zealand. (p. 24). Geological Society of New Zealand Miscellaneous Publication 119A.

Elkink, A. (2010). Retaining walls. *Build Magazine*, *120*, 25–26.

Elkink, A. (2016). Low retaining walls. *Build Magazine*, *152*, 26–29.

EQC. (2015). *1 Wallis Road, Inner Kaiti, Gisborne Geotechnical Investigation Report, 29820.7979-GIR*. Earthquake Commission.

Fellows, D. L., & Barker, N. (2021). Slope failures, scour and infrastructure damage: Tairāwhiti road network response to multiple severe weather events. New Zealand Geotechnical Society Symposium, 24–26 March, Dunedin, pp. 1–8.

Fookes, P. G., Lee, E. M., & Milligan, G. C. (2005). *Geomorphology for engineers*. Whittles.

Franks, C. A. M. (1988). Engineering Geological Assessment of the impact of Cyclone Bola March 1988 on the damline & dam extension line sections of the Gisborne City water supply. EG88/011.

Funning, G. J., & Garcia, A. (2016). A systematic study of earthquake detectability using Sentinel-1 Interferometric Wide-Swath data. *Geophysical Journal International*, *216*, 332–349.

Glade, T. (1998). Establishing the frequency and magnitude of landslide triggering rainstorm events in New Zealand. *Environmental Geology*, *35*, 160–174.

Hancox, G. T., & Wright, K. (2005). Analysis of landsliding caused by the 15–17 February 2004 rainstorm in the Wanganui-Manawatu hill country, southern North Island, New Zealand. GNS Science Report 2005/11, p 64.

Hearn, G. J., Hunt, T., & D'Agostino, S. (2011). C3 soil slope stabilization. *Geological Society of London, Engineering Geology Special Publication*, *24*, 165–188.

Hungr, O., Leroueil, S., & Picarelli, L. (2014). The Varnes classification of landslide types, an update. *Landslides*, *11*, 167–194.

Keim, R. F., Tromp-van Meerveld, H. J., & McDonnell, J. J. (2006). A virtual experiment on the effects of evaporation and intensity smoothing by canopy interception on subsurface stormflow generation. *Journal of Hydrology*, *327*, 352–364.

Kluger, M. O., Jorat, M. E., Moon, V. G., Kreiter, S., de Lange, W. P., Mörz, T., Robertson, T., & Lowe, D. J. (2020). Rainfall threshold for initiating effective stress decrease and failure in weathered tephra slopes. *Landslides*, *17*, 267–281.

Li, N., & Cheng, Y. M. (2015). Laboratory and 3-D distinct element analysis of the failure mechanism of a slope under external surcharge. *Natural Hazards and Earth System Sciences*, *15*, 35–43.

Li, S., Xu, W., & Li, Z. (2022). Review of the SBAS InSAR Time-series algorithms, applications, and challenges. *Geodesy and Geodynamics*, *13*, 114–126.

MacManus, J. (2021). Gisborne floods: State of emergency lifted as water levels recede. https://www.stuff.co.nz/national/weather-news/126897175/gisborne-floods-state-of-emergency-lifted-as-water-levels-recede

Marden, M. (2004). Future-proofing erosion-prone hill country against soil degradation and loss during large storm events: Have past lessons been heeded? *New Zealand Journal of Forestry*, *49*, 11–16.

Massey, C. I., Townsend, D. B., Lukovic, B., Morgenstern, R., Jones, K. E., Rosser, B. J., & de Vilder, S. J. (2020). Landslides triggered by the 14 November 2016 Mw 7.8 Kaikoura earthquake: An update. *Landslides*, *17*, 2401–2408.

Mazengarb, C. (1997). *Slope instability and mud volcano hazard assessment, Gisborne District Council. Client Report, 44692d. 13A*. Institute of Geological & Nuclear Sciences.

Mazengarb, C., & Speden, I. G. (2000). *Geology of the Raukumara area. 1:250,000 Geological Map 6*. Institute of Geological & Nuclear Sciences.

McKelvey, R. J., & Murton, K. (1991). Landslide damage on the East Coast region arising from tropical cyclone bola, March 1988. In D. H. Bell (Ed.), *Landslides* (Vol. 1, pp. 1445–1450). Balkema.

Neef, G., Watters, W. A., & Edwards, A. R. (1996). The mid-Castlecliffian Mangatuna formation of the Gisborne district,

North Island, New Zealand. *New Zealand Journal of Geology and Geophysics*, *39*, 551–558.

NIWA. (2023). Climate Summary for January 2023. https://niwa.co.nz/climate/monthly/climate-summary-for-january-2023

Notti, D., Herrera, G., Bianchini, S., Meisina, C., García-Davalillo, J. C., & Zucca, F. (2014). A methodology for improving landslide PSI data analysis. *International Journal of Remote Sensing*, *35*, 2186–2214.

Olshansky, R. B. (1998). Regulation of hillside development in the United States. *Environmental Management*, *22*, 383–392.

Ozturk, U., Bozzolan, E., Holcombe, E. A., Shukla, R., Pianosi, F., & Wagener, T. (2022). How climate change and unplanned urban sprawl bring more landslides. *Nature*, *608*, 262–265.

Ram, A. R., Brook, M. S., & Cronin, S. J. (2018). Geomorphological characteristics of slope failures in Northeast Viti Levu Island, Fiji, triggered by Tropical Cyclone Winston in February 2016. *New Zealand Geographer*, *74*, 64–76.

Rogers, N., McDougall, N., Teal, J., Thomas, M., & Soysa, S. (2022). Drought prone buildings-an unmitigated disaster in waiting. *New Zealand Geomechanics*, *104*, 62–68.

Rosser, B. J., & Wolter, A. (2022). New data on the large Whareongaonga landslide. GeoNet News. https://www.geonet.org.nz/news/5mcQ5GIU6EEJVpwabBcALz#:~:text=The%20volume%20of%20sediment%20deposited,sea%20by%20approximately%2050%20m

Samsonov, S., Dille, A., Dewitte, O., Kervyn, F., & D'Oreye, N. (2020). Satellite interferometry for mapping surface deformation time series in one, two and three dimensions: A new method illustrated on a slow-moving landslide. *Engineering Geology*, *266*, 105471.

Schwarz, M., Giadrossich, F., & Cohen, D. (2013). Modeling root reinforcement using a root-failure Weibull survival function. *Hydrology and Earth System Science*, *17*, 4367–4377.

Sharma, A. (2023). Cyclone Gabrielle: Gisborne homes red-stickered, water supply critical, residents asked to avoid travel on roads. New Zealand Herald 15 February. https://www.nzherald.co.nz/nz/cyclone-gabrielle-gisborne-water-crisis-residents-warned-of-taps-running-dry-mayors-plea-to-save-water/KU33HXKI7NEI7L3LHK6KT5VJJE/

Sidle, R. C., & Ochiai, H. (2006). *Landslides – processes, prediction, and land use*. Water resources monograph series. American Geophysical Union.

Skempton, A. W. (1964). Long term stability of clay slopes. *Géotechnique*, *14*, 77–101.

Stringer, J., Brook, M. S., & Justice, R. (2021). Post-earthquake monitoring of landslides along the Southern Kaikōura Transport Corridor, New Zealand. *Landslides*, *18*, 409–423.

Tan, L. (2023). Weather: Cyclone Hale – widespread flooding, slips and evacuations; Gisborne/Tairāwhiti declares state of emergency. New Zealand Herald 11 January. https://www.nzherald.co.nz/nz/weather-cyclone-hale-widespread-flooding-slips-and-self-evacuations-north-island-communities-bracing-for-more-wild-weather/3JTCNNKYQZDFFGLBLGLUG5DJYU/

Wasowski, J., & Bovenga, F. (2014). Investigating landslides and unstable slopes with satellite Multi Temporal Interferometry: Current issues and future perspectives. *Engineering Geology*, *174*, 103–138.

Wood, J. (2021). Cantilever pole retaining walls. *New Zealand Geomechanics News*, *101*, 16–60.

Xu, Q. J., & Zhang, L. M. (2010). The mechanism of a railway landslide caused by rainfall. *Landslides*, *7*, 149–156.

Zhang, D., Yang, W., Xu, C., Ye, T., & Liu, Q. (2022). Extracting deforming landslides from time-series Sentinel-2 imagery. *Landslides*, *19*, 2761–2774.

Zhang, Y. J., Fattahi, H., & Amelung, F. (2019). Small baseline InSAR time series analysis: Unwrapping error correction and noise reduction. *Computers and Geosciences*, *133*, 104331.

How to cite this article: Cook, M., Brook, M., & Cave, M. (2023). Interferometric Synthetic Aperture Radar (InSAR) and field-based observations of rainfall-triggered landslides from the November 2021 storm, Gisborne/Tairāwhiti, New Zealand. *New Zealand Geographer*, *79*(2), 138–152. https://doi.org/10.1111/nzg.12373